論 文
36～3～5

입력보상 및 최적출력 PIM제어를 적용한 스위칭 직류변환기의 제어기 설계

A Controller Design for Switching Regulator Using an Optimal Output PIM Control with Feedforward Comensation

高 政 鎬*・權 鳳 煥*・尹 明 重**
(Jung-Ho Ko, Bong-Hwan Kwon, Myung-Joong Youn)

Abstract

This paper describes a design method for the buck type switching regulator to improve transient and steady state performances. Necessary design considerations on the power stage are given before designing the controller to obtain better transient responses with less control effort and a feedforward compensation is also given to effectively improve the steady state performance. In the design of the controller, a PIM (proportional-integral-measurable) control method with optimized constant feedback gains is presented to get better tansient and steady state performances without complicating the implementation of controller. Computer simulations and experimental results are given to show the usefulness of the presented technique.

1. Introduction

In the past decade, a great deal of researches on the switched mode DC to DC converter (switching regulator) has been done to obtain a practical tool for analysis 1)～7) and to improve its performances as the increasing demands of the switching power supply. In these researches, the results are maninly based on the conventional frequency domain analysis 7)～16). However, these methods can not directly handle the design of the feedback compenstor with optimized feedback gains. Futhermore, it is rather difficult to predict the closed loop output responses in the time domain, especially when the output transient performances are important design specifications. In the design of the controller, proportional control method of the output error with proper compensation in the frequency domain has been widely used for the simplicity of implementation 12)～14). But these methods generally result in the deficiencies of performances. In recent researches, a current mode control method has been introduced to improve performances of the system 15)～16). However, in the practical applications, there still exist some problems such as the complexity of the controller and difficulties in the current sensing.

Among the several topologies of the swithing regulators, buck (step down) type topology has some advantages over the other topologies due to the typical characteristics of high efficiency, low output ripple, and simple structure easy to control. In this paper, therefore, a design method of the optimal output PIM (proportional—integral—measurable) controller for the buck type swithing regulator is presented to satisfy the dy-

*正會員：韓國科學技術院 電氣 및 電子工學科 博士課程
**正會員：韓國科學技術院 電氣 및 電子工學科 教授・工博
接受日字：1986年 9月 9日
1次修正：1986年 11月 13日

namic performances in the time domain without complicating the implementation of the controller and a feed-forward control method is also given to improve the steady state performance under the situation of the nonideal DC input to the switching regulator. Futhermore, necessary design considerations on the power stage are given to obtain a better closed—loop transient responses with less control effort under the constraint of the permissible switching ripple. In the optimization of the controller parameters, a design technique using the time weighted quadratic performance index is proposed to obtain a better transient output responses rather than those based on the conventional quadratic performance index. The computer simulations and experimental results are also given to show the usefulness of the presented techniques.

2. Power Stage Design

2.1 Design problem formulation

To satisfy the steady state performance requirements of the buck type switching regulator, both the characteristics of the power stage and that of the controller should be considered. Since the inherent switching ripple components of the output voltage can not be generally removed by the feedback controller, small bandwidth of the low pass filter (LPF) is required to reduce the switching ripple component of the output voltage. However, small bandwidth of the LPF will result in the poor dynamic characteristics, thus we are faced with the trade off problem between the steady state switching ripple magnitude and the transient performance of the output voltage. In the design of the power stage parameters, the following design problems can be formulated to satisfy the conditions discussed above.

1) Bandwidth of the LPF should be selected as wide as possible under the constraint of the permissible switching ripple.

2) Care must be taken to prevent the series resonant frequencies from coinciding with the significant frequencies contained in the input DC voltage source inherently.

3) In the possible operating duty ratio, the converter should operate on the continuous conduction mode.

2.2 Characteristics of the power stage

In order to satisfy the power stage design problems formulated in the previous section, the characteristics of the power stage should be investigated. As shown in Fig. 1, 4th order power stage gives wider bandwidth than 2nd order power stage under the condition of the same attenuation ratio at the switching frequency. In the following, 4th order LPF scheme is chosen and analyzed for the power stage of the buck type switching regulator.

The magnitude of the transfer function of the power stage in the frequency domain is calculated easily as follows:

$$|H(jw)| = 1/[p(w)]^{\frac{1}{2}} = 1/[p_1^2(w)+p_2^2(w)]^{\frac{1}{2}} \qquad (1)$$

where,

$$p_1(w)=aw^4-cw^2+1, \qquad p_2(w)=w(d-bw^2)$$

$$a=C_1'C_2'L_1'L_2', \qquad b=C_1'L_1'L_2'$$

$$c=C_1'L_1'+C_2'L_1'+C_2'L_2', \qquad d=L_1'+L_2'.$$

In the above equation, w denotes angular frequency and C_1', C_2', L_1' and L_2' are normalized parameters with respect to load resistor R as follows;

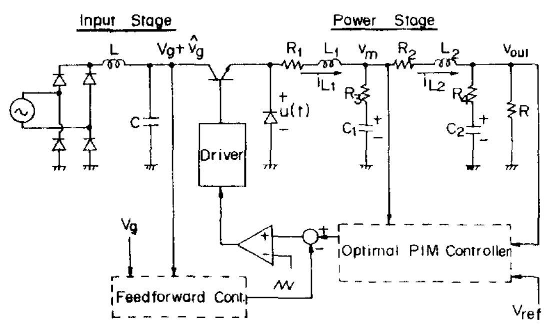

Fig. 1 Circuit digram of the buck type switching regulator (R_1, R_2, R_3, R_4: Effective series resistance of inductor and capacitor.)

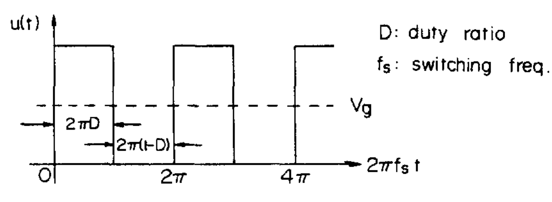

Fig. 2 Waveform of the input voltage to the power stage (in case of continuous conduction mode operation)

$$C_1'=C_1R,\ C_2'=C_2R,\ L'=L_1/R,\ L_2'=L_2/R \quad (2)$$

Since there is the degree of the freedom in the determination of the parameters, some constraints are given on the normalized parameters as follows;

$$C_1'=C_2'=C',\ L_1'\geq L_2'. \quad (3)$$

To find resonant frequencies, one can obtain the following significant frequencies by equating $p_1(w)$, $p_2(w)$, $\dot{p}_1(w)$, $\dot{p}_2(w)$ to zero respectively;

$$w_1\cong\sqrt{1/[C'(2L_1'+L_2')]} \quad (4)$$
$$w_2\cong\sqrt{(2L_1'+L_2')/(C'L_1'L_2')}$$
$$w_3=\sqrt{(L_1'+L_2')/(C'L_1'L_2')} \quad (5)$$
$$w_4=\sqrt{(2L_1'+L_2')/(2C'L_1'L_2')} \quad (6)$$
$$w_5=\sqrt{(L_1'+L_2')/(3C'L_1'L_2)}. \quad (7)$$

From (4) to (7), the following inequalities can easily be derived:

$$w_1<w_5<w_4<w_3<w_2. \quad (8)$$

In order to find the ranges of resonant ferquencies at which p(w) locally minimized, the derivatives of the p(w) for w_1 through w_5 are calculated using the relation of $\dot{p}(w)=2p_1(w)\dot{p}_1(w)+2p_2(w)\dot{p}_2(w)$ as follows;

$$\dot{p}(0)=0 \quad (9\text{-a})$$
$$\dot{p}(w_1)>0 \quad (9\text{-b})$$
$$\dot{p}(w_2)>0 \quad (9\text{-c})$$
$$\dot{p}(w_3)<0 \quad (9\text{-d})$$
$$\dot{p}(w_4)<0 \quad (9\text{-e})$$
$$\dot{p}(w_5)>0. \quad (9\text{-f})$$

It is easily known that one of the local minimunm frequencies exists between w_3 and w_2. To find one more local minimum frequency left, the values of p(0) and $p(w_1)$ is calculated as:

$$p(0)=1 \quad (10\text{-a})$$
$$p(w_1)=p_1^2(w_1)+p_2^2(w_1)=p_2^2(w_1)=w_1^2(d-bw_1^2)^2 \quad (10\text{-b})$$

In the above equations, $p(w_1)$ is nearly zero provided that the following condition holds. This condition is believed to be appropriate except for the case of extremely heavy—duty loads;

$$C'>>3L_1'. \quad (11)$$

Since p(w) is a function of 8th order with even symmetry, the resonant frequencies (w_{r1}, w_{r2}) of the power stage are obtained from (8), (9) and (10) as follows:

$$w_3<w_{r1}<w_2 \quad (12\text{-a})$$
$$w_{r2}\approx w_1 \quad (12\text{-b})$$

Next, in the following, an important condition on the operation mode of the converter is to be considered. The input waveform to the power stage shown in Fig. 2 is valid in case of the continuous conduction mode. However, a practical converter may operate on the discontinuous conduction mode unintentionally, which generally causes severe ripple problem. To prevent the converter from operating on this mode, it is necessary to satisfy the following condition for continuous conduction mode 3)~4);

$$L_1>R(1-D)/(2f_s) \quad (13)$$

where D and f_s denote steady state duty ratio and switching frequency, respectively.

2.3 Design procedure.

Using the resonant frequencies and the condition for the continuous conduction mode, the following inequalities are obtained to satisfy the design problems;

$$w_{r1,max}=w_2=\sqrt{(2L_1'+L_2')/(C'L_1'L_2')}<2\pi f_1^* \quad (14)$$
$$w_{r2}\approx w_1=\sqrt{1/[C'(2L_1'+L_2')]}>2\pi f_2^* \quad (15)$$
$$(1-D)/(2f_s)<L_1'<1/(2f_s) \quad (16)$$

In (14), $w_{r1,max}$ denotes maximum possible value of the resonant frequency and in the following, f_1^* can be obtained to satisfy the design problem 1) discussed proviously. The maximum peak to peak switching ripple magnitude is derived using the peak to peak magnitude of the fundamental component of u(t) and transfer property of the power stage as follows;

$$V_{s,pp,max}=\frac{4V_g}{\pi}\ |H(j2\pi fs)|\ =\frac{4V_g}{\pi}(f_1^*/f_s)^4 \quad (17)$$

and the permissible switching ripple is also given by multiplying the constant r to the total output ripple desired as follows;

$$V_{s,per.} = r \cdot (\%\, r_i\, pple) \cdot D \cdot V_g/100. \tag{18}$$

By equating (17) and (18), f_1^* is determined as follows;

$$f_1^* = [r \cdot \pi \cdot (\%\, \text{ripple}) \cdot D/400]^{\frac{1}{4}} f_s \tag{19}$$

where, 0.1~0.5 is used as the value of r which depends on the designer's choice as a rule of thumb. In (15), f_2^* is selected to meet the design problem 2) as follows;

$$f_2^* = \alpha\beta N f \tag{20}$$

where, generally 2~5 is used as the value of α to prevent significant frequency contained in the rectified DC input form coinciding with resonent frequencies, N is the number of phase (N=1 for single phase, N=3 for three phase), f is the frequency of AC input, and β is 1 for the half wave rectifier and 2 for full wave rectifier. Finally, in (16), the upper range of L_1' is obtained by setting the steady state duty ratio zero for the possible operating range of the switching regulator. The permissible ranges of the power stage parameters are shown in Fig. 3 as the shaded area. Futhermore, for design purpose, the maximum permissible ranges of L_2' and C' are approximately given from (3), (14) and (15) when L_1' is predetermined by (16) as follows;

$$3/(4\pi^2 f_1^{*2} L_1') < C' < 1/(8\pi^2 f_2^{*2} L_1') \tag{21}$$

$$4L_1'/[(f_1^*/f_2^*)^2 - 2] < L_2' \le L_1'. \tag{22}$$

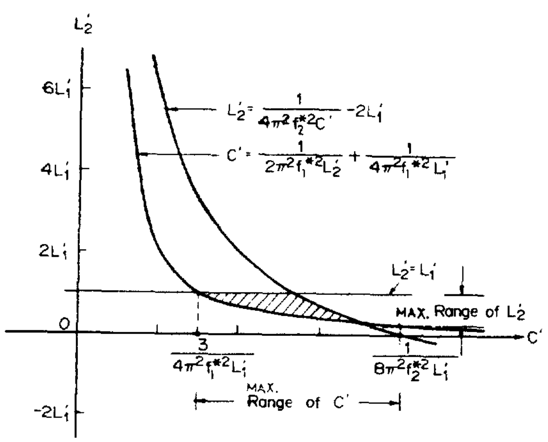

Fig. 3 Permissible ranges of the parameters of the power stage

3. Controller Design

3.1 Modelling of the buck type switching regulator

It is is assumed that the converter shown in Fig. 1 operates in the continuous conduction mode with the parameters chosen as previously stated. To obtain an analytical tool for analysis, the state space averaging concept has been adopted 1)~2). With the choice of the state vector,

$$x(t) = [V_m(t)\ \ V_{out}(t)\ \ i_{L1}(t)\ \ i_{L2}(t)]^T \tag{23-a}$$

the state equations are obtained by

$$\dot{x}(t) = A\, x(t) + B\, u(t) \tag{23-b}$$

$$y(t) = C\, x(t) \tag{23-c}$$

$$y_m(t) = C_m x(t) \tag{23-d}$$

where

$$A = \begin{bmatrix} -R_3(1/L_1 + 1/L_2 & R_3/L_2 & 1/C_1 - R_1R_3/L_1 & R_2R_3/L_2 - 1/C_1 \\ RR_4/[L_2(R+R_4)] & \dfrac{-R(R_4/L_2 + 1/RC_2)}{(R+R_4)} & 0 & \dfrac{R(1/C_2 - R_2R_4/L_2)}{(R+R_4)} \\ -1/L_1 & 0 & -R_1/L_1 & 0 \\ 1/L_2 & -1/L_2 & 0 & -R_2/L_2 \end{bmatrix}$$

$$B = [R_3/L_1\ \ 0\ \ 1/L_1\ \ 0]^T$$

$$C = [\ 0\ \ 1\ \ 0\ \ 0]$$

$$C_m = [\ 1\ \ 0\ \ 0\ \ 0]$$

the state vector, where, $y(t)$ and $y_m(t)$ denote voltage and measurable output voltage respectively and A, B, C, and C_m have the proper dimensions as described above.

3.2 Feedforward compensation

In this section, necessary design considerations on the improvement of the steady state performance (output ripple) are given in the following. The ripple component contained in the practically nonideal DC input source can be thought as disturbance term and must be reduced effectively. Although a great majority of the disturbance can be reduced by the effect of the feedback controller provided that the closed loop dynamics is much faster than the unknown disturbance, the magnitude of the reduced ripple component contained in the output voltage, in the practical applications, may often be considered unsatisfactory. An effective compensation technique, therefore, is required to obtain the improved steady state performances. In order to do so, a feedforward control concept is now introduced as shown in Fig. 4. In this figure, the disturbance ($\hat{v}_g$) can be cancelled out by subtracting the effective mangnitude from the control signal entering the input terminal of the pulse width modulation (PWM) amplifier. This type of the feedforward compensator is easily implemented using the operational amplifier and passive elements.

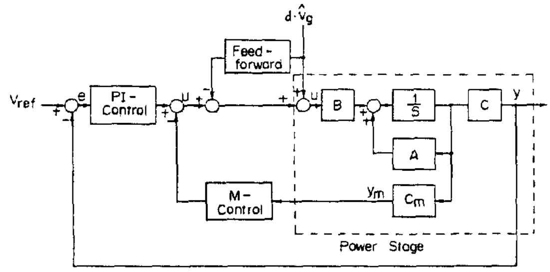

Fig. 4 Block diagram of the closed loop system

3.3 Control problem formulation

When a step reference voltage $y_s(=V_{ref})$ is added to the buck type switching regulator, the output voltage $y(=V_{out})$ is desired to track y_s with no steady state error and the minimum time is also desired to reach the stady state condition with a reasonable overshoot under the limitation of bounded input voltage. In order to meet both the performance requirements and the ease of implemention effectively, we consider the following PIM controller:

$$u(t)=k_i z(t)-k_P[y(t)-y_s(t)]-k_m y_m(t) \tag{24}$$

where the subscript s denotes steady state, $z(t)=y(t)-y_s(t)$, $z(0)=0$, and k_i, k_P, and k_m are constant feedback gains to be determined. This type of controller provides no steady state error for a step response by the integral action of the output error and better dynamic response is also expected using the measurable variable. We take the time weighted quadratic performance index of the form,

$$J=\int_0^{\infty} [t^k(y-y_s)'Q(y-y_s)+(u-u_s)'r_1(u-u_s)]dt \tag{25}$$

to emphasize both the transient responses and the practical limitation of the bounded input problem. In (25), prime denotes transpose, Q and r_1 are the symmetric positive definite matrices, and u_s and y_s the steady state input to the power stage and the steady state desired output (V_{ref}), respectively. The time weighted quadratic performance index is of prime importance rather than the conventional quadratic performance index (k=0 case in (25)) especially when the sustained error of the output are expected. The control problem is now to be formulated as finding the constant feedback gains of the output PIM control law which minimizes the time weighted quadratic performance index J under the situation of no disturbance in the input by the feedforward compensation.

3.4 Optimal constant feedback gains

In the steady state with no output error, steady state values of the states and input are derived from

$$\begin{bmatrix} x_s \\ u_s \end{bmatrix} = \begin{bmatrix} A & B \\ C & 0 \end{bmatrix}^{-1} \begin{bmatrix} 0 \\ y_s \end{bmatrix} \tag{26}$$

where $u_s=-k_i z_s-k_m y_{ms}$. Using the variables $\bar{x}=x-x_s$, $\bar{u}=u-u_s$, $\bar{y}=y-y_s$, $\bar{y}_m=y_m-y_{ms}$, $\bar{z}=z-z_s$, we can obtain the following equations:

$$\dot{\bar{x}}=A\bar{x}+B\bar{u},\ \bar{x}(0)=-x_s \tag{27-a}$$

$$\bar{y}=C\bar{x} \tag{27-b}$$

$$\bar{y}_m=C_m\bar{x} \tag{27-c}$$

$$\dot{\bar{z}}=\bar{y}=C\bar{x},\ \bar{z}(0)=-z_s \tag{27-d}$$

where

$$z_s=-k_i^{-1}u_s-k_i^{-1}k_m y_{ms}. \tag{28}$$

Now, we define the new control input v and the augmented state vector w,

$$w=[\bar{z}^T\ \bar{x}^T]^T,\ v=\bar{u}. \tag{29}$$

Then, the augmented system is described as

$$\dot{w}=\bar{A}w+\bar{B}v, \tag{30}$$

$$v=-K\bar{C}w \tag{31}$$

where

$$\bar{A}=\begin{bmatrix}0 & C\\ 0 & A\end{bmatrix},\ \bar{B}=\begin{bmatrix}0\\ B\end{bmatrix},\ w(0)=\begin{bmatrix}-z_s\\ -x_s\end{bmatrix},$$

$$K=[k_i\ k_P\ k_m],$$

$$\bar{C}=\begin{bmatrix}I_{r\times r} & 0\\ 0 & C\\ 0 & C_m\end{bmatrix}$$

and the performance index is expressed as follows

$$J=\int_0^\infty (t^k w^T\bar{Q}w + w^T\bar{C}^T K^T r_1 K\bar{C}w)dt \tag{32}$$

where

$$\bar{Q}=\mathrm{diag}(O_{r\times r},\ C^TQC).$$

Using the procedure presented in 17)~19), the necessary conditions for feedback gain matrix K to be optimal with respect to the performance index (32) is given by

$$dJ/dK=2[-\bar{B}^T\sum_{i=1}^{k+1}P_iL_i+r_1K\bar{C}L_{k+1}]\bar{C}^T$$
$$-2k_i^{-T}[(I_{r\times r},\ O_{r\times n})P_{k+1}\begin{bmatrix}z_s & z_s^T\\ x_s & z_s^T\end{bmatrix},\ O_{r\times r},\ (I_{r\times r},$$
$$O_{r\times n})P_{k+1}\begin{bmatrix}z_s & x_s^T\\ x_s & x_s^T\end{bmatrix}C_m^T]=0, \tag{33}$$

where P_i and L_i satisfy the following equations:

$$(\bar{A}-\bar{B}K\bar{C})^T P_1+P_1(\bar{A}-\bar{B}K\bar{C})+\bar{Q}=0$$

$$(\bar{A}-\bar{B}K\bar{C})^T P_{i+1}+P_{i+1}(\bar{A}-\bar{B}K\bar{C})+P_i=0,\ (i=1,\ 2,\ldots\ldots,\ k-1)$$

$$(\bar{A}-\bar{B}K\bar{C})^T P_{k+1}+P_{k+1}(\bar{A}-\bar{B}K\bar{C})+P_k+\bar{C}^T\bar{K}^T r_1 K\bar{C}=0$$

$$(\bar{A}-\bar{B}K\bar{C})\ L_i+L_i(\bar{A}-\bar{B}K\bar{C})^T+L_{i+1}=0,\ (i=1,\ 2,\ldots\ldots,k)$$

$$(\bar{A}-\bar{B}K\bar{C})\ L_{k+1}+L_{k+1}(\bar{A}-\bar{B}K\bar{C})^T+w(0)\ w(0)^T=0.$$

Then, the final cost becomes

$$J=w(0)^T\ P_{k+1}\,w(0).$$

In the above equation (33), state vector x, input vector u, output vector y, and measurable output vector y_m are assumed as n, r, r and p dimensional vector, respectively.

4. A design example and experimental results

Using the same nomenclature previously stated, it is assumed that the design specifications are given as follows

f_s=15kHz, %ripple=0.05, R=10Ω, D=0.5,
full wave rectified input stage,
Ac input: 60Hz, single phase.

If we choose $\alpha=2.5$ and $r=0.1$, then f_1^*=999Hz, f_2^*=300Hz from (19) and (20) respectively. From (2) and (16), the range of L_1 is obtained as

$$167\mu H<L_1<333\mu H$$

and maximum ranges of L_2 and C are determined from (2), (19) and (20) with L_1 being 300μH as follows:

$$254\mu F<C<469\mu F.$$

These ranges of parameters satisfy the condition (11) sufficiently. The frequency response of the power stage for the selected parameters is simulated and showm in Fig. 5 where it is noted that the equation (12) is well satisfied.

In the computer simulations of the converter using the PIM controller, the following performance index is used,

$$J=\int_0^\infty[(t/tr)^k\ \bar{y}^2+r_1\bar{u}^2]dt \tag{34}$$

where k is positive integer. Then, the weighting matrix $\bar{Q}$ becomes as

$$\bar{Q}=\mathrm{diag}(0,0,(1/tr)^k,0,0) \tag{35}$$

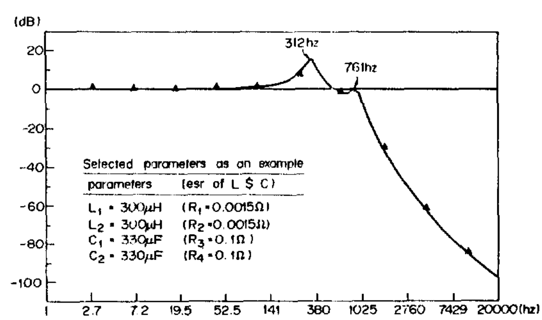

Fig. 5 Frequency response of the power state for the parameters selected as an example

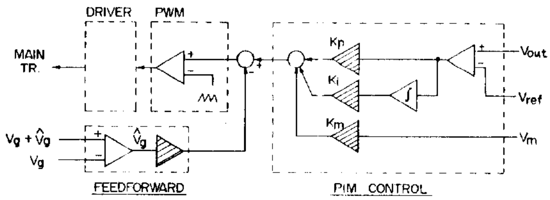

Fig. 6 Circuit diagram of the controller

where tr in (34) is used to give relatively larger weighting on the sustained output error square after rising time expected. The circult diagram of the PIM controller with feedforwad compensator is given in Fig. 6. In this figure, the controlled signal activates main switching transistor through the pulse width modulator and transistor driving circuit. According to the optimal gains derived from the proposed algorithm as shown in Table 1, the transient and steady state responses of the output are simulated and experimented as shown in Fig. 8 through 10. As shown in Table 1, 5% settling time of output response using the time weighted quadratic performance

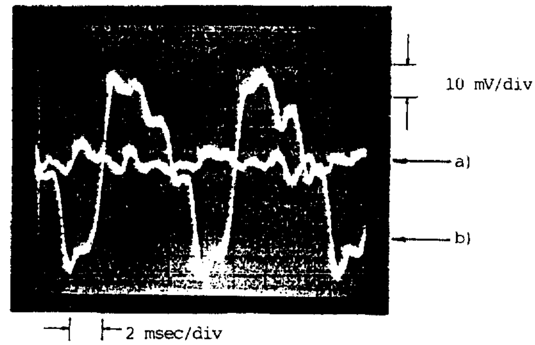

Fig. 7 Steady state output responses (ripple)
a) with feedforward compensation
b) without feedforward compensation

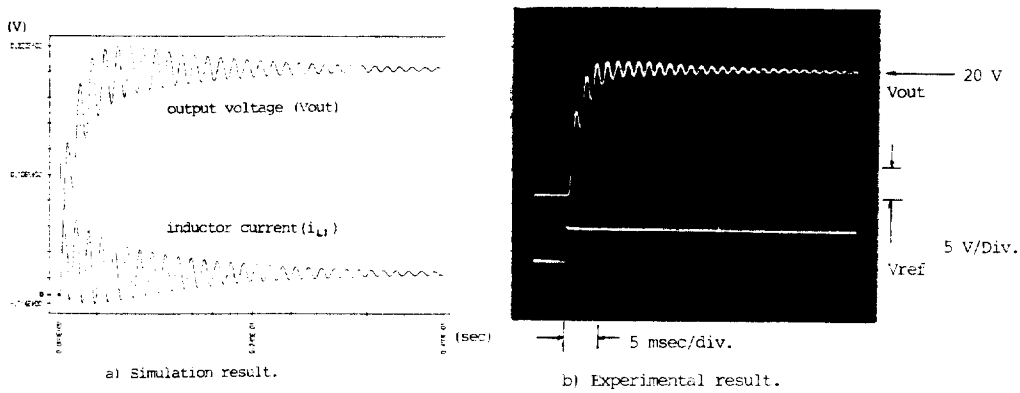

Fig. 8 Transient responses of the closed loop system (in case of k=0)

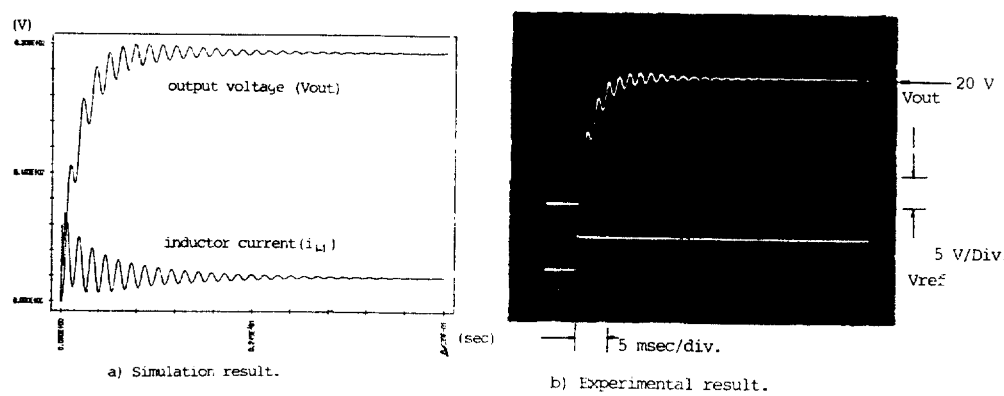

Fig. 9 Transient responses of the closed loop system (in case of k=2)

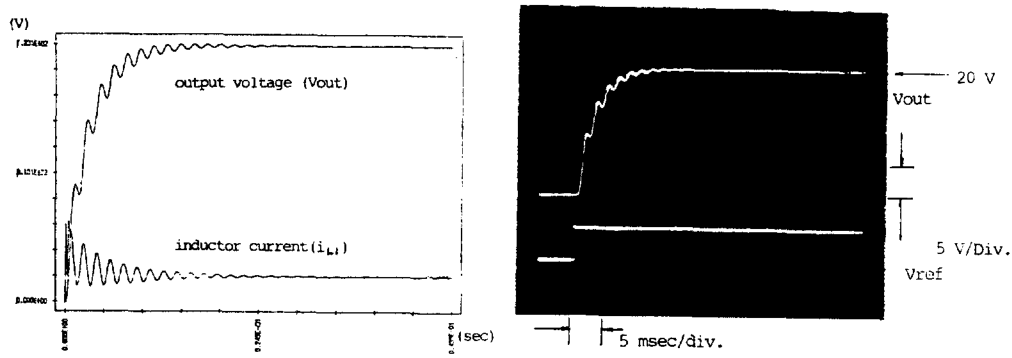

a) Simulation result.

b) Experimental result.

Fig. 10 Transient responses of the closed loop system (in case of k=5)

index (k=2, 5) is shorter than that of using the conventional quadratic performance index (k=0) due to the oscillatory response. Futhermore, from the controlled inductor waveforms, it can be considered that the continuous conduction mode operation is well guaranteed as already expected in the power stage design. The effect of feedforward controller is also presented experimentally as shown in Fig. 7 where the steady state output ripple is shown to be reduced significantly. Thus, it is shown that the experimental results well satisfy the theoretical buck type switching regulator.

Table 1. Optimal constant gains and settling times

time weighting index (k)	tr	r	optimal gains ki	kp	km	settling time (msec)
0	0.005	0.2	7211	1.91	11.7	22
2	0.005	0.2	8931	1.00	18.3	10
5	0.005	0.2	6827	1.12	18.8	9.3

5. Conclusion

This paper has investigated a design method of the buck type switching regulator to improve transient and steady state performances. The parameters of the power stage has been analytically determined before designing the controller to get better tansient responses with less control effort. A design method of an output PIM controller with optimized constant feedback gains has been presented without complicating the controller by using the measurable variable, and a feedforward compensation has also been given to improve steady state performance in a simple manner. As shown in the design example, steady state output ripple has also significantly been reduced from 60 msec to 10 msec using the feedforward compensation, and 5% settling times of output responses are 9.3 msec for k=5, 10 msec for k=2, and 22 msec for k=0 respectively. Thus, it is believed that better transient responses have been obtained using the time weighted quadratic performance index and the usefulness of the proposed design method which covers the design of controller as well as power stage has been proved by the computer simulations and experimental results.

References

1) R.D. Middlebrook and S. Cuk, "A General Unified Approach to Modelling Switching Converter Power Stages", IEEE PESC Record, 76CHO 1084-3AES, pp.18-34, 1976.

2) W.M. Polivka, P.R.K Chetty, and R.D. Middlebrook, "State Space Average Modelling of Converters with Parastics and Storage Time Modulation", IEEE PESC Record, pp.98-104, 1980.

3) S. Cuk and R.D. Middlebrook, "A General Unified Approach to Modelling Switched Mode DC to DC Converters in Discontinuous Conduction Mode", IEEE PESC Record, 1977.

4) R.D. Middlebrook and S. Cuk, "Modelling and Analysis Methods for DC to DC Switching Converters", IEEE International Semiconductor Power Converter Conference, 1977 Record, 77CH 1183-

3IA, pp.90–111.

5) Y.S. Lee, "A Systematic and Unified Approach to Modelling Switches in Switched Mode Power Supply", IEEE Trans. Industr. Elec, Vol IE–32, NO.4, pp.445–448, 1985.

6) G.C. Verghes, M.E. Elbuluk and J.G. Kassakian, "A General Approach to Sampled–Data Modelling for Power Electronic Circuits", IEEE Trans. Power Electronics, Vol.PE–1, No.2, April 1986.

7) Y. Yu, F.C. Lee and Joseph Kolecki, "Modelling and Analysis of Power Processing System", IEEE RESC Record, 79CH 1461–3, pp.11–24, 1979.

8) F. Barzegar, S. Cuk and R.D. Middlebrook, "Using Small Computers to Model and Measure Magnitude and Phase of Regulator Transfer Functions and Loop Gain", Proceedings of Powercon 8, 1981.

9) R. Mahadevan, S. El–Hamamsy, W.M. Polivka and S. Cuk, "A Converter with Three Switched–Networks Improves Regulation, Dynamics and Control", Proceedings of Powercon 10, E–1, pp.1–17, 1983.

10) H.D. Venerable, "The k Factor: A New Mathematical Tool for Stability Analysis and Synthesis", Proceedings of Powercon 10, H–1, pp.1–12, 1983.

11) R.D. Middlebrook, "Predicting Modulator Phase Lag in PWM Converter Feedback Loops", Proceedings of Powercon 8, H–4, pp.1–6, April 1981.

12) S. Cuk, "General Topological Properties of Switching Structures", IEEE PESC Record, 79CH 1461–3, pp.109–130, 1979.

13) K. Harada and T. Nabeshima, "Large–signal Transient Response of Switching Regulator", IEEE PESC Record, 81CH 1652–7, pp.388–394, 1981.

14) H.A. Nienhaus and D.E. Palmar, "Automatic Fault Diagnosis of A Switching Regulator", IEEE PESC Record, 81CH1652–7, pp.154–165, 1981.

15) B. E. Andersen, et.al, "Analysis of the Static Characteristics and Dynamic Response of Push–pull Switching Converters Operating in the Current Programmed Mode", IEEE PESC Record, pp.29–38, 1981.

16) Richard Redl and Istvan Novak, "Instabilities in Current–mode Controlled Switching Regulator", IEEE PESC Record, 81CH1652–7, pp.17–28, 1981.

17) B.H. Kwon, M.J. Youn and Z. Bien, "Optimal Constant Feedback with Time Multiplied Performance Index for discrete–time Linear Systems", IEEE Trans. Automatic Control, Vol.AC–30, No.5, pp.497–498, 1985.

18) Satoru Fukata, Akira Mohri and Masaru Takara, "Optimization of Linear System with Integral Control for Time–weighted Quadratic Performance Index", Int. J. Control, Vol.37, No.5, pp.1057–1070, 1983.

19) B.H. Kwon, "A Study on the Optimal Output Feedback Controller and Observer Using Time–multiplied Performance Index", M.S. Thesis, KAIST, 1984.